Preliminary Experimental Evaluation of In-Situ Calibration Methods for MEMS-based Attitude Sensors and Doppler Sonars in Underwater Vehicle Navigation

Giancarlo Troni and Louis L. Whitcomb

***Abstract*— We report preliminary results of an in-water test-tank experimental evaluation of recently reported methods for the problem of *in-situ* calibration of the alignment rotation matrix between Doppler sonar velocity sensors and attitude sensors arising in the navigation of underwater vehicles. Unlike previous reports employing high-cost high-accuracy attitude sensors, including true-North-seeking gyrocompasses and high-precision accelerometers, we address the case of using attitude sensing with a low-cost Micro-electro-mechanical systems (MEMS) attitude and heading reference system. We report a comparative experimental evaluation of several recently reported calibration methods when employing low-cost MEMS attitude sensors. The methods are experimentally evaluated using data obtained with the Johns Hopkins University (JHU) remotely operated underwater vehicle in the JHU Hydrodynamic Test Facility. We report the preliminary results of comparative analysis of the performance of recently reported calibration methods and a most previously technique indicating satisfactory performance of the proposed methods for the problem of *in-situ* calibration of the alignment rotation matrix between Doppler sonar velocity sensors and low-cost MEMS-based attitude sensors.**

I. Introduction

Oceanographic exploration is advancing dramatically due to improvements in precision underwater navigation. These developments have made possible underwater missions that were previously considered impractical or infeasible (e.g. [4], [6]). Doppler sonar navigation, perhaps the most commonly employed method for high-precision near-bottom vehicle navigation, typically employs a 3-axis Doppler velocity log (DVL), a precision pressure depth sensor, and a 3-axis attitude and heading reference system (AHRS) sensor. Although there are several sources of error that limits Doppler navigation precision, previous studies have reported that the accuracy of the calibration of the alignment between the AHRS and the DVL can be a significant (and even dominant) source of navigation error, e.g. [2], [7], [10], [13], [25].

Several previously reported calibration alignment methods employ information from external sensors such as the global positioning system (GPS), ultra short baseline (USBL) navigation systems, and long-baseline (LBL) acoustic navigation systems. In [8], Joyce reports a heading alignment estimation based on least squares and GPS information. In [2], [3], Brokloff reports a least-squares technique using GPS for estimating the 3-axis alignment between the attitude sensor and the DVL. GPS is unavailable for deeply submerged vehicles, however, so absolute acoustic navigation methods such as long-baseline or ultra-short baseline acoustic navigation systems can be employed, but these methods require additional navigation sensors and/or beacons to be located external to the underwater vehicle on the sea floor or on a surface ship. In [12], the authors report using LBL information and a least-square techniques to estimate the 3-axis DVL/AHRS alignment, and in [11], report a method for the problem based on adaptive identification on the group of rigid-body rotations. In [18], the authors report a formulation of this approach based on the use of rotors in geometric algebra. Alternative methods are originally reported in [21] employing attitude data, acceleration data, and Doppler sonar velocity data to perform DVL/AHRS calibration. This approach is extended to incorporate the use of depth sensor data, and evaluated with in-laboratory experimental vehicle data in [22] and with at-sea data in [20]. An advantage of this approach over previous methods is that no sensors external to the vehicle, e.g. GPS, USBL, or LBL, are required.

Low-cost Micro-electro-mechanical systems (MEMS)-based attitude sensors estimate vehicle attitude with less precision and are more affected by external disturbances than

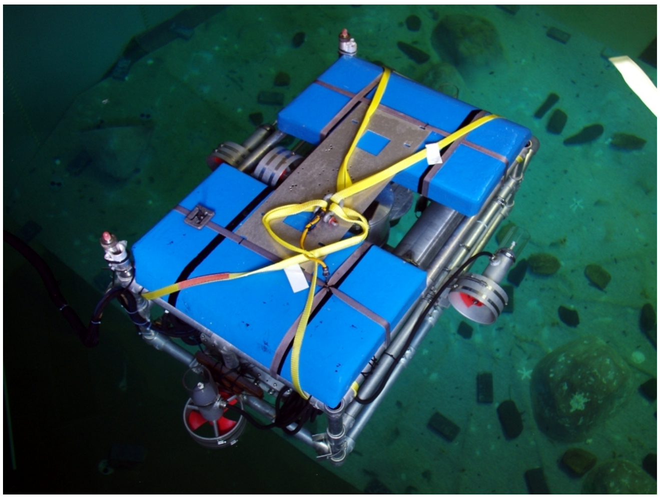

Fig. 1. Johns Hopkins University (JHU) remotely operated vehicle (ROV) inside the JHU Hydrodynamic Test Facility

This work was supported by the National Science Foundation under NSF award IIS-0812138. Support for the first author was also provided by a Fulbright/Conicyt Fellowship.

The authors are with the Department of Mechanical Engineering, Johns Hopkins University, Baltimore, MD 21218, USA. Email: {gtroni,llw}@jhu.edu

are high-accuracy attitude sensors such as true-North-seeking optical gyrocompasses and inertial navigation systems (INS). To estimate pitch and roll, low-cost MEMS-based attitude sensors are normally instrumented with accelerometers that are orders of magnitude less sensitive than the accelerometers normally employed in the high-accuracy attitude sensors. To estimate heading, normally MEMS-based attitude sensors employ magnetometers that are affected by external magnetic disturbances. In some MEMS AHRS units, MEMS angular rate sensors are also employed, in addition to magnetometers and accelerometers, for the estimation of heading, pitch, and roll. The principal advantages of some of the previously reported methods for DVL/AHRS alignment calibration are that they do not require sensor data obtained with external navigation beacons, and one of these methods does not require full precise attitude information, and thus they may be suitable for use with less expensive underwater vehicles instrumented with low-cost attitude sensors such as MEMS AHRS units.

In this paper we report the results of a comparative experimental analysis of the performance of three previously reported DVL/AHRS calibration methods with navigation data obtained with the Johns Hopkins University (JHU) remotely operated vehicle (ROV) underwater vehicle in the JHU Hydrodynamic Test Facility shown in Figure 1. The results reveal consistent differences in performance of the various DVL/AHRS calibration methods when analyzed on navigation data from several different in-water experiments.

This paper is organized as follows: In Section II we give a brief overview of Doppler navigation and the DVL and AHRS alignment calibration problem. In Section III we report previously proposed methods to solve this problem. In Section IV we describe the experimental setup. In Section V we report the results of a comparative analysis to evaluate the performance of the previously reported methods using MEMS-based attitude sensors. Section VI summarizes and concludes.

II. Background

This section briefly reviews basic concepts of Doppler navigation.

A. Notation

For each vector, a leading superscript indicates the frame of reference and a following subscript indicates the sensor source, thus ${}^{w}p_l$ is the LBL position in the world coordinates, ${}^{v}v_d$ is the Doppler velocity sensor in the vehicle frame and ${}^{i}a_i$ is the accelerometer linear acceleration in the inertial sensor frame.

The set of 3×3 rotation matrices forms a group, known as the special orthogonal group, SO(3), defined as

$$SO(3) = \{R : R \in \mathbb{R}^{3\times3}, R^T R = I, det(R) = 1\}. \quad (1)$$

For each rotation matrix a leading superscript and subscript indicates the frames of reference. For example, ${}^{w}_{v}R$ is the rotation from the vehicle frame to the world frame.

B. Overview of Doppler Navigation

A Doppler navigation sonar measures the instrument's three-axis velocity with respect to the fixed sea floor. The most common Doppler sonar configuration for underwater vehicle navigation consists of four downward-looking acoustic transducers each oriented at 30° from the instrument vertical axis. Each transducer measures acoustically the velocity of the instrument parallel to its beam with respect to the fixed sea floor [17]. The four beam velocity measurements vector $v_b(t)$ is linearly mapped to a Cartesian instrument frame ${}^{d}v_d(t) \in \mathbb{R}^3$, and a normalized error measurement $e(t) \in \mathbb{R}^1$, by a static 4×4 instrument transformation matrix $T \in \mathbb{R}^{4\times4}$:

$$\begin{bmatrix} {}^{d}v_d(t) \\ e(t) \end{bmatrix} = T\ v_b(t). \quad (2)$$

The instrument velocity in the world frame based on the Doppler velocity sensor is given by

$${}^{w}v_d(t) = {}^{w}_{v}R(t)\ {}^{v}_{d}R\ {}^{d}v_d(t), \quad (3)$$

where ${}^{v}_{d}R$ is the constant rotation matrix from instrument coordinate frame to the vehicle coordinate frame, and ${}^{w}_{v}R(t)$ is the time varying rotation matrix from the vehicle coordinate frame to the inertial world coordinate frame. In practice, ${}^{v}_{d}R$ is often difficult or impossible to measure accurately on an actual underwater vehicle. This paper addresses the problem of estimating the unknown ${}^{v}_{d}R$ using commonly available *in-situ* navigation data.

The world frame velocity can be integrated to obtain a dead-reckoned DVL position estimation ${}^{w}p_d(t)$ [25], by

$${}^{w}p_d(t) = {}^{w}p_d(t_0) + \int_{t_0}^{t} {}^{w}v_d(\tau)\, d\tau. \quad (4)$$

III. Review of Calibration Methods

We consider an underwater vehicle with the following three commonly used navigation sensors:

1. **DVL**: A bottom-lock Doppler sonar providing 3-axis linear velocities, ${}^{d}v_d(t)$, defined in (3).
2. **AHRS** providing absolute attitude represented by ${}^{w}_{v}R(t)$ and comprised of at least of:
   - 2.1. **Gyroscopes**: A 3-axis gyroscope providing angular velocity vector ${}^{v}\omega_v \in \mathbb{R}^3$.
   - 2.2. **Accelerometers**: A 3-axis accelerometer providing linear acceleration vector ${}^{i}a_i(t) \in \mathbb{R}^3$.
3. **Depth Sensor**: Vehicle depth, ${}^{w}d_v(t)$, computed from pressure measurements using standard equations, e.g. [5].

The goal is to use data from these sensors to calibrate the unknown alignment rotation matrix, ${}^{v}_{d}R$, between the AHRS and the Doppler sonar.

To solve the *in-situ* alignment calibration problem, the present authors proposed methods (velocity-based and acceleration-based) and reported simulation, laboratory and at-sea studies of these methods [20]–[22] for the case of high accuracy attitude sensors. The present paper reports an evaluation and comparison of the methods proposed in [20]–[22]

for the case of MEMS-based attitude sensors using in-water laboratory data from the JHU ROV. The remainder of this section reviews these previously reported approaches. A full analysis takes into account the sensors location offsets, but without loss of generality and for simplicity of exposition, in this review we assume that the Doppler transducer origin is co-located with the accelerometer and AHRS sensor origin at the origin of the vehicle reference frame. We assume the depth sensor is co-located or compensated to Doppler sonar origin. Additionally, the vehicle coordinate frame axes are coincident with the attitude sensor frame axes.

A. ISVD Method

For comparison pruposes we will use the ISVD method that it requires data from an external position sensor (LBL, USBL) to estimate the rotation matrix from the following equation:

$$ {}^{v}_{w}R(t)\,{}^{w}p_l(t) - \int {}^{v}_{w}\dot{R}(\tau)\,{}^{w}p_l(\tau)\,d\tau = {}^{v}_{d}R(t) \int {}^{d}v_d(\tau)\,d\tau. \quad (5) $$

A direct method to solve the unknown constant rotation matrix ${}^{v}_{d}R$ in (5) from experimental data using a singular value decomposition (SVD) approach is reported in [1], [24]. For a more detailed discussion of the ISVD method, the reader is referred to [12].

B. Velocity-based Method

Integrating the acceleration data from the accelerometers and comparing these with the velocity from the Doppler sonar, we obtain

$$ {}^{w}_{v}R(t)^{\top} \int_{t_0}^{t} {}^{w}_{v}R(\tau)\,{}^{v}a_v(\tau)\,d\tau + {}^{v}v_v(t_0) = {}^{v}_{d}R\,{}^{d}v_d(t), \quad (6) $$

where we assume that the initial vehicle velocity, ${}^{v}v_v(t_0)$, is known. To improve the performance of this methods we added data from the depth sensor. The vertical coordinate of the Doppler frame origin is given by

$$ {}^{w}d_d(t) = e_3^{\top}\,{}^{w}p_d(t), \quad (7) $$

where $e_3 = [0\,0\,1]^{\top}$ and ${}^{w}d_d(t)$ is the scalar representing the depth of the Doppler frame origin. Differentiating (7) and using (3) we obtain

$$ {}^{w}\dot{d}_d = e_3^{\top}\,{}^{w}_{v}R(t)\,{}^{v}_{d}R\,{}^{d}v_d(t). \quad (8) $$

To estimate the constant unknown matrix ${}^{v}_{d}R$ we combine the equation (6) with (8). We add the depth equation (8) to the velocity-based equation (6) that can be solved for the unknown ${}^{v}_{d}R$ using a gradient descent optimization method to minimize the sum of squared errors constrained to $SO(3)$. For a more detailed discussion of the velocity-based method, the reader is referred to [20]–[22]. We denote this solution as ${}^{v}_{d}R_{VEL-DE}$.

C. Acceleration-based Method

Taking the time derivative of (6) results in

$$ {}^{v}a_v = {}^{v}\hat{W}_v\,{}^{v}_{d}R\,{}^{d}v_d + {}^{v}_{d}R\,{}^{d}\dot{v}_d, \quad (9) $$

where ${}^{v}\hat{W}_v$ is the skew-symmetric tensor of the angular velocity in the vehicle frame computed by the attitude sensor. (9) can be solved from experimental data for the unknown ${}^{v}_{d}R$ using a gradient descent optimization to minimize the sum of squared errors constrained to $SO(3)$. Similarly, we can add (8) to the acceleration-based equation (9) that can again be solved with a constrained to $SO(3)$ minimization method. For a more detailed discussion of the acceleration-based method, the reader is referred to [20]–[22]. We denote this solution as ${}^{v}_{d}R_{ACC-DE}$.

IV. Performance Evaluation

The proposed methods were experimentally evaluated using data obtained with the JHU ROV, Figure 1, in the JHU Hydrodynamic Test Facility [9]. This Section gives an overview of the experimental setup.

A. Experimental Setup

The facility contains a 7.5 m diameter and 4 m deep indoor fresh water tank. The JHU ROV displaces 150 Kg and is actuated by six 1.5 kW DC brushless electric thrusters. The vehicle is capable of actively being controlled in 6 degrees of freedom (DOF). A suite of sensors commonly employed in deep submergence underwater vehicles is present on the JHU ROV. Table I specifies the navigation sensors employed in this study.

TABLE I

JHU ROV Navigation Sensors Precision and Update Rate

Instrument	Model	Variable	Specification	Update Rate
AHRS	Microstrain 3DM-GX3-25 [14]	Attitude Angular Rate Acceleration	$\pm 2°$ $0.03°/s/\sqrt{h}$ $0.08mg/\sqrt{h}$	100 Hz
DVL	Teledyne RDI 1200 kHz [19]	Velocity	$\pm 0.2\%$ ± 1 mm/s	8 Hz
Pressure sensor	Paroscientific [16]	Depth	0.01%	15 Hz
LBL	Marquest Sharps 300 kHz LBL System	XY Position	5 mm	5 Hz

We note that the measured LBL sensor data rate and precision employed herein is higher than those commonly available on underwater vehicles. As the new proposed methods do not require LBL information, the experimental performance of the proposed new methods will not be affected, but the high quality LBL data will improve the performance of the previously reported method in [12] that is used for comparison purposes. DVLNAV navigation software was used to log all sensor data [10].

The data were re-sampled to a uniform sampling interval of 10 Hz. The Doppler velocity, AHRS attitude, and angular velocity are used in these experiments without any extra processing or filtering. The acceleration data is reported by the AHRS including local gravity vector. The gravity vector is removed using the AHRS attitude pitch and roll. The calculated acceleration data are scaled with the local gravitational constant and the mean is removed to reduce the effects of the gravity vector estimation and finally filtered with an acausal (forward and backward) first order low-pass filter with 2 Hz cutoff frequency. The LBL fix data outliers were manually removed. The time-derivative of depth is required for some of the methods proposed. The raw depth data were numerically differentiated and filtered with an acausal (forward and backward) first order low-pass filter with 1 Hz cutoff frequency.

There are several limitations for this performance evaluation. In this study we focus on reducing the systematic errors due to inaccurate knowledge of the alignment between the AHRS and the DVL. There are several other sources of errors (non-orthogonality, scale factors, biases) that affect the performance of the dead-reckoning position estimation, but these errors are beyond the scope of the present study.

One of the specific limitations for this study is that all the experiment were performed in a $195\ \mathrm{m}^3$ steel water tank. The steel tank is a very challenging environment for heading estimation with magnetometers. To reduce the effect of the magnetic distortions, a magnetic calibration was performed reducing the heading errors due to magnetic disturbances from several tens of degrees of error to less than five degrees in heading. Under this circumstances the performance results of this study can be considered to be under more challenging magnetic conditions than at-sea. More details about the performance of the MEMS-based attitude sensors on Doppler-based navigation in this specific location can be found in [23].

The AHRS employed in this study, a Microstrain 3DM-GX3-25 [14], estimates attitude (heading, pitch, and roll) in real-time with a complementary filter employing data from the unit's 3-axis magnetometer, 3-axis accelerometer, and its 3-axis angular rate sensors. Most MEMS angular-rate sensors are affected by a bias offset that changes with time and temperature and, in consequence, they are often provided with a calibration procedure to correct the observed angular-rate sensor bias. We observed with this model AHRS that an uncorrected bias offset in the angular rate sensors will cause a bias in the resulting estimated attitude. Figure 2 shows the attitude estimated in real-time by the AHRS's complementary filter in the presence of uncorrected angular-rate sensor bias and the attitude we estimated in post-processing using only accelerometer and magnetometer data. These data show a mean difference between the two attitude estimates of of $+1.59^\circ$ in heading, -0.03° in pitch and -1.99° in roll. This internal AHRS bias error, if uncorrected, is a significant impediment for the problem of calibrating the DVL/AHRS alignment. In these experiments, the angular-rate sensor bias was corrected at the beginning of each experiment by calculating a 30 second average of the angular-rate sensor output while the vehicle was motionless. Correcting the angular-rate sensor bias was observed to reduce the AHRS reported attitude bias by an order-of-magnitude.

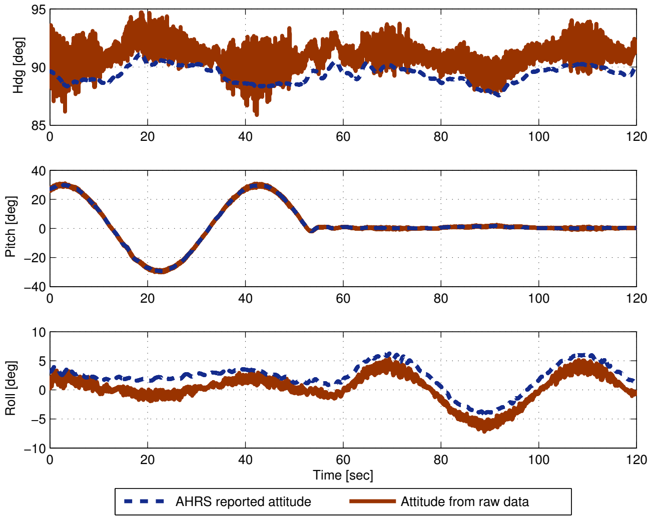

Fig. 2. Attitude reported by the AHRS sensor and the calculated from raw measurements from the magnetometers and accelerometers. All angles in degrees.

B. Experiments Description

The training experiments are designed to calibrate DVL/AHRS alignment. These experiments consist in a sequence of sinusoidal movements in X, Y, and Z axis. Figure IV-B shows a section of the XYZ position of the vehicle during JHU ROV experiment T1. The validation experiments are designed to evaluate the performance of each previously estimated solution by comparing the estimated position with the "ground truth" LBL position. These experiments are designed to represent a rectangular seafloor survey mission. Figure IV-B shows the three dimensional visualization of the XYZ position of the vehicle during JHU ROV experiment V1. Table II and III summarize the duration and distance traveled of the four training experiments and two validation experiments respectively used in this study. The system controller was performing in closed loop trajectory tracking for each trajectory.

TABLE II
TRAINING EXPERIMENTS PARAMETERS

Experiment	T1	T2	T3	T4
Survey Duration	62 min	63 min	46 min	18 min
Track line Distance	606.1 m	752.0 m	456.2 m	113.4 m

TABLE III
VALIDATION EXPERIMENTS PARAMETERS

Experiment	V1	V2
Survey Duration	35 min	43 min
Track line Distance	149.9 m	129.1 m

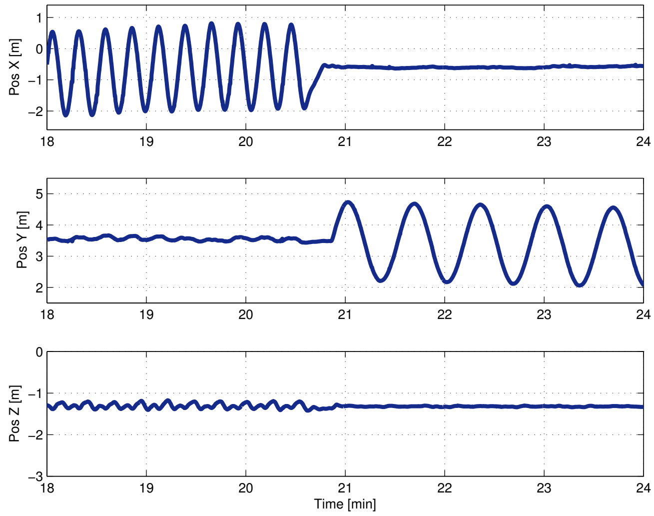

Fig. 3. JHU ROV XYZ trajectory for experiment T1. All distances in meters.

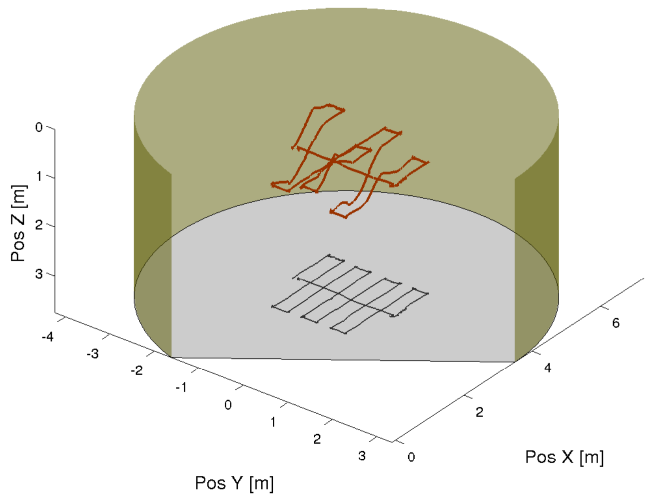

Fig. 4. JHU ROV three dimensional trajectory for experiment V1. All distances in meters.

C. Evaluation Methodology

We compare the performance of the following five alignment calibration methods.

a. *Manual*: A manually measured alignment matrix, denoted as ${}^v_d R_{MANUAL}$. In JHU ROV, the Doppler sensor is mounted with a known alignment offset of $+45.0^\circ$ in heading and $+0.0^\circ$ in pitch and roll.
b. *Loose*: For comparison purposes a manually selected alignment matrix, denoted as ${}^v_d R_{LOOSE}$, representing a less accurate measurement of the alignment offset defined as $+46.0^\circ$ in heading and $+1.0^\circ$ in pitch and roll.
c. *ISVD*: A previously reported method utilizing LBL navigation fix information as described in Section III-A that is used for comparison purposes. The solution obtained is denoted as ${}^v_d R_{ISVD}$. The ISVD method is implemented removing the mean of the sensor data, ${}^w p_l(t)$, as well as the mean of the left and right hand side terms in the estimation equation.
d. *AVE-DE*: The velocity-based combined with the depth-based method as described in Section III-B we obtain the solution denoted as ${}^v_d R_{AVE-DE}$.
e. *ACC-DE*: The acceleration-based method combined with the depth-based method as described in Section III-C we obtain the solution denoted as ${}^v_d R_{ACC-DE}$.

To measure the performance of each method, we calculate the following quantities:

a. *Position error metric*: Using the alignment estimate resulting from each method we recomputed the Doppler track of the vehicle, ${}^w p_d(R)$, using (4). We evaluated the performance of each method by comparing the estimated position with the "ground truth" LBL position, ${}^w p_l$, and calculate the standard deviation,

$$\hat{\sigma} = [\hat{\sigma_x}\, \hat{\sigma_x}\, \hat{\sigma_x}]^\top = \sigma(p_l -^w p_d(R)) \qquad (10)$$

and a position error metric (PE) is defined as

$$||\vec{\sigma}||_2 = (\sigma_x^2 + \sigma_y^2 + \sigma_z^2)^{\frac{1}{2}}. \qquad (11)$$

b. *Geodesic distance metric*: An alternative measurement is used to evaluate the quality of the solutions. Using (12) to calculate the geodesic distance, as in [15], between the estimated rotation matrix, R, and the best estimate to the real value, $\hat{R}$. In this case we will use ${}^v_d R_{MANUAL}$ as the "ground truth" and best estimation of the real value ${}^v_d R$ given by

$$d_g(R, \hat{R}) = \frac{180}{\pi} ||log(R^\top \hat{R})||_2 \qquad R, \hat{R} \in SO(3). \qquad (12)$$

c. *Percentage of distance traveled*: Using the standard dead-reckoning navigation metric reporting the error of the final position as a percentage of the distance traveled (DT).

V. Results

This section reports a comparative evaluation of the performance of three different *in-situ* calibration methods as described in Section III.

For all the experiments the performance is very similar if we use the same experiment to estimate and validate the performance for these cases. Although the method ISVD shows in general the best results. Figure 5 shows the position error for experiment T1 using the same experiment for estimation.

Figure 6 shows the error between the XYZ LBL measured position and the integrated dead-reckoned DVL position estimation calculated using (4) based on each of the estimated alignment matrices. Table IV shows the alignment angles estimates in Euler angles representation of the methods discussed in Section III using experiment T1 for estimation and experiment V1 for validation. The Table includes for

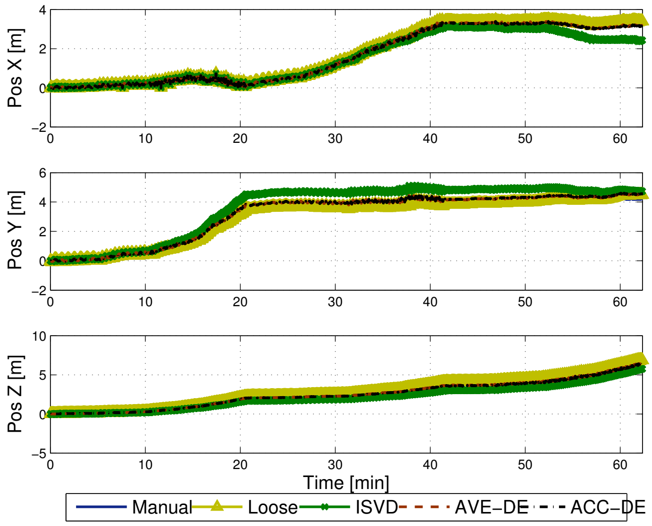

Fig. 5. Laboratory Experiments XYZ Position Error: Position error correspond to DVL renavigated position minus the "ground truth" LBL measured position. Self validation for experiment T1. Each color represent the solution to one of the proposed methods.

each method the geodesic distance to the manually measured alignment matrix, the position error metric and the percentage of DT detailed in previous section. Best performance in each column is marked in bold.

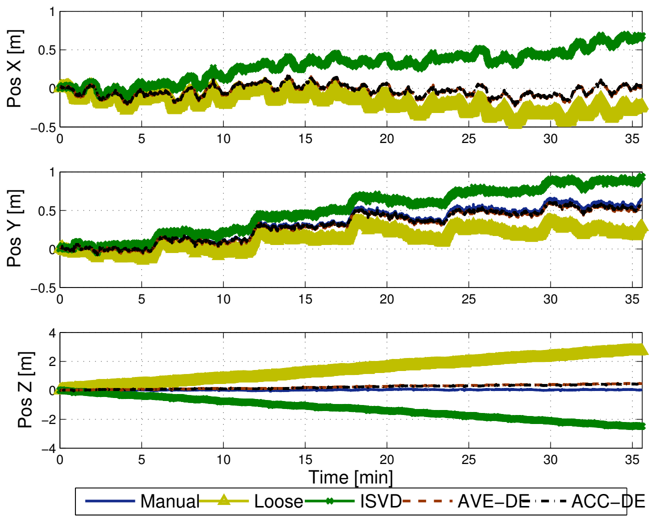

Fig. 6. Laboratory Experiments XYZ Position Error: Position error correspond to DVL renavigated position minus the "ground truth" LBL measured position. Cross validation using experiment T1 for estimation and experiment V1 for validation. Each color represent the solution to one of the proposed methods.

Examination of the position error in the performance results, Table IV, shows that all the methods give a reasonable answer under these evaluation conditions. In general, the one of the best performance is from the manual estimation, as in this case the alignment calibration offset is known. But for the case of a manually measured value with an error of 1 $^\circ$ in each axis, called the loose method, the results are not satisfactory. Performance from AVE-DE and ACC-DE methods are as good as the Manual method performance, and in some cases better, making them good alternatives in cases where the manual alignment calibration is not available. Under these evaluation conditions, the worst performance in position error is found in the ISVD method. This is a consequence of the fact that the ISVD method is affected by the drift in the error position due to others sources of errors different than the error in the alignment of the DVL and AHRS.

Figure 7 shows the position error distributions for experiment T1/V1. This figure indicates that for several proposed methods the error is almost always less than 80 cm, i.e. in a 35 min experiment traveling 150 m, the error is in the range of 0.5% of the distance traveled.

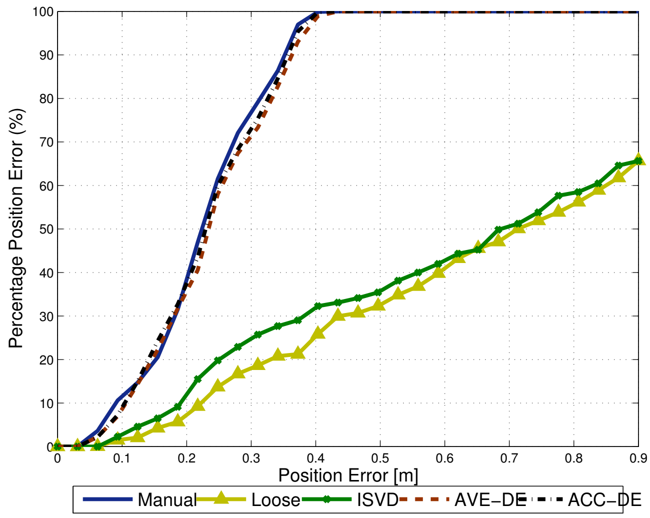

Fig. 7. Position Error Distribution. Cross validation using experiment T1 for estimation and experiment V1 for validation. The y-axis shows the percentage of the position error that was under certain threshold (x-axis).

Figure 8 show the percentage of DT error performance for all four estimation experiments and evaluated each in the two validation experiments for a total of eight cases evaluated for each method. Error bars show the distribution of the values for each method. Figure 8 confirms that on average the results are in the same range to the case analyzed of experiments T1/V1.

The results show that the AVE-DE and ACC-DE methods have accuracy better than the accuracy of previously reported methods for the case of using MEMS-based attitude sensors. In general the AVE-DE method shows better performance than ACC-DE method, but for some cases is possible to estimate more accurate the alignment with the ACC-DE. The new methods require only data available from on-board vehicle sensors, and this may be more practical and convenient to employ at sea in comparison to methods requiring external navigation beacons.

TABLE IV

SUMMARY OF THE PERFORMANCE EVALUATION RESULTS FOR ESTIMATION USING EXPERIMENT T1 AND USING THE EXPERIMENT V1 TO EVALUATE THE PERFORMANCE. BEST PERFORMANCE IN EACH COLUMN IS MARKED IN BOLD.

-	Heading	Pitch	Roll	SO3 Dist	σ_x	σ_y	σ_z	$\|\|\vec{\sigma}\|\|_2$	%DT XYZ
Manual	45.000	-0.000	0.000	0.000	0.109	0.215	**0.024**	**0.242**	**0.468**
Loose	46.000	1.000	1.000	1.727	0.116	**0.131**	0.795	0.814	1.908
ISVD	44.213	-3.631	1.846	4.137	0.195	0.293	0.719	0.801	1.904
AVE-DE	44.843	-0.619	0.967	**1.158**	0.074	0.197	0.140	0.253	0.516
ACC-DE	44.507	-0.668	0.987	1.288	**0.072**	0.198	0.129	0.247	0.506

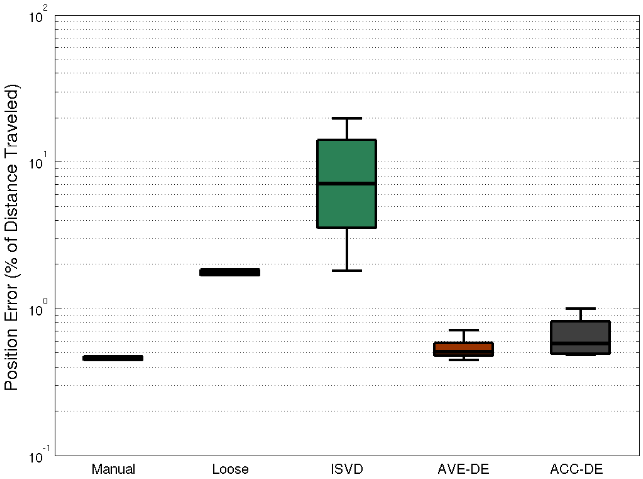

Fig. 8. Position error as a percentage of the distance traveled of each method for different experiments. Each box plot is calculated from four different estimation experiments evaluated with two different trajectories.

VI. CONCLUSIONS

This paper reports a comparative performance evaluation, using in-water data from the JHU ROV underwater vehicle, of three methods (ISVD, AVE-DE and ACC-DE) for the problem of *in-situ* calibration of the alignment rotation matrix between Doppler sonar velocity sensors and MEMS-based attitude sensors arising in the navigation of underwater vehicles. Our results indicate satisfactory performance of the methods, AVE-DE and ACC-DE, not requiring external position in the presence of real sensor noise of actual in-water navigation conditions. The AVE-DE method is shown to offer the best calibration performance over the ensemble of six experiments analyzed herein. But for some specific training experiments the ACC-DE method is shown to offer an accurate estimation. The ISVD method requires the availability of absolute position fixes, e.g. from a LBL or USBL navigation system, but does not require instrumentation of acceleration. Conversely, the ACC-DE and AVE-DE methods require the instrumentation of acceleration, but does not require absolute position fixes from a LBL or USBL navigation system, making suitable for the case of vehicles instrumented with low-cost less-accurate attitude sensors. These data indicate the practical utility of these calibration methods for the commonly occurring situation in which accurate *a-priori* manual Doppler sonar and MEMS-based attitude sensors calibration is impractical or infeasible.

ACKNOWLEDGMENT

The authors would like to thank Christopher McFarland and Michael Brown for their help in improving and maintaining of JHU ROV.

REFERENCES

[1] K. S. Arun, T. S. Huang, and S. D. Blostein. Least-squares fitting of two 3-D point sets. *IEEE Trans. Pattern Anal. Mach. Intell.*, 9(5):698–700, 1987.

[2] N. A. Brokloff. Matrix algorithm for Doppler sonar navigation. In *OCEANS 1994*, volume 3, pages III/378 –III/383 vol.3, 13-16 1994.

[3] N. A. Brokloff. Dead reckoning with an ADCP and current extrapolation. In *OCEANS 1997*, volume 2, page 1411 vol.2, 6-9 1997.

[4] R. Camilli, C. Reddy, D. Yoerger, B. Van Mooy, M. Jakuba, J. Kinsey, C. McIntyre, S. Sylva, and J. Maloney. Tracking hydrocarbon plume transport and biodegradation at Deepwater Horizon. *Science*, 330(6001):201, 2010.

[5] N. P. Fofonoff and R. C. Millard. Algorithms for computation of fundamental properties of seawater. *UNESCO Technical Papers in Marine Science*, 44:53, 1983.

[6] C. R. German, A. Bowen, M. L. Coleman, D. L. Honig, J. A. Huber, M. V. Jakuba, J. C. Kinsey, M. D. Kurz, S. Leroy, J. M. McDermott, B. M. de Lépinay, K. Nakamura, J. S. Seewald, J. L. Smith, S. P. Sylva, C. L. Van Dover, L. L. Whitcomb, and D. R. Yoerger. Diverse styles of submarine venting on the ultraslow spreading Mid-Cayman Rise. *Proceedings of the National Academy of Sciences*, 107(32):14020–14025, 2010.

[7] B. Jalving, K. Gade, K. Svartveit, A. Willumsen, and R. Sørhagen. DVL velocity aiding in the HUGIN 1000 integrated inertial navigation system. *Modeling, Identification and Control*, 25(4):223–236, 2004.

[8] T. M. Joyce. On in situ calibration of shipboard ADCPs. *Journal of Atmospheric and Oceanic Technology*, 6(1):169–172, 1989.

[9] J. C. Kinsey, D. A. Smallwood, and L. L. Whitcomb. A new hydrodynamics test facility for UUV dynamics and control research. In *OCEANS 2003*, volume 1, pages 356–361 Vol.1, 2003.

[10] J. C. Kinsey and L. L. Whitcomb. Preliminary field experience with the DVLNAV integrated navigation system for oceanographic submersibles. *Control Engineering Practice*, 12(12):1541–1549, 2004.

[11] J. C. Kinsey and L. L. Whitcomb. Adaptive identification on the group of rigid-body rotations and its application to underwater vehicle navigation. *Robotics, IEEE Trans. on*, 23(1):124–136, Feb. 2007.

[12] J. C. Kinsey and L. L. Whitcomb. In situ alignment calibration of attitude and Doppler sensors for precision underwater vehicle navigation: Theory and experiment. *Oceanic Engineering, IEEE Journal of*, 32(2):286–299, April 2007.

[13] R. McEwen, H. Thomas, D. Weber, and F. Psota. Performance of an AUV navigation system at Arctic latitudes. *Oceanic Engineering, IEEE Journal of*, 30(2):443–454, April 2005.

[14] Microstrain Inc. 3DM-GX3-25 miniature attitude heading reference system datasheet. Technical Report P/N 8400-0033 rev. 002, Microstrain Inc., Williston, VT, 2012.

[15] F. C. Park. Distance metrics on the rigid-body motions with applications to mechanism design. *J. Mech. Des.*, 117(1):48–54, 1995.

[16] Paroscientific Inc. Submersible depth sensors series 8000. Technical report, Paroscientific Inc., Redmond, WA, 2005.

[17] RD Instruments Inc. Acoustic Doppler current profilers principals of operation: A practical primer (2nd edition). Technical Report P/N 951-6069-00, RD Instruments Inc, San Diego, CA, 1996.

[18] M. J. Stanway and J. C. Kinsey. Sensor alignment using rotors in geometric algebra. In *Robotics and Automation (ICRA), 2011 IEEE International Conference on*, pages 994 –999, May 2011.

[19] Teledyne RD Instruments Inc. Workhorse navigator DOPPLER VELOCITY LOG (DVL). Technical report, RD Instruments Inc, Poway, CA, 2011.

[20] G. Troni, J. Kinsey, D. Yoerger, and L. Whitcomb. Field performance evaluation of new methods for in-situ calibration of attitude and Doppler sensors for underwater vehicle navigation. In *Robotics and Automation (ICRA), 2012 IEEE International Conference on*, pages 5334 –5339, may 2012.

[21] G. Troni and L. L. Whitcomb. New methods for *In-Situ* calibration of attitude and Doppler sensors for underwater vehicle navigation: Preliminary results. In *OCEANS 2010*, pages 1–8, Seattle, WA, Sept. 2010.

[22] G. Troni and L. L. Whitcomb. Experimental evaluation of new methods for in-situ calibration of attitude and Doppler sensors for underwater vehicle navigation. In *Intelligent Robots and Systems (IROS), 2011 IEEE/RSJ International Conference on*, pages 3722 –3727, sept. 2011.

[23] G. Troni and L. L. Whitcomb. Experimental evaluation of a MEMS inertial measurements unit for Doppler navigation of underwater vehicles. *OCEANS 2012*, october 2012. To Appear.

[24] S. Umeyama. Least-squares estimation of transformation parameters between two point patterns. *IEEE Trans. Pattern Anal. Mach. Intell.*, 13(4):376–380, 1991.

[25] L. L. Whitcomb, D. Yoerger, and H. Singh. Advances in Doppler-based navigation of underwater robotic vehicles. In *IEEE Int. Conf. on Robotics and Automation.*, volume 1, pages 399–406 vol.1, 1999.